Electrochemistry Communications 119 (2020) 106814

Contents lists available at ScienceDirect

Electrochemistry Communications

journal homepage: www.elsevier.com/locate/elecom

An electrochemical investigation of oxygen adsorption on Pt single crystal electrodes in a non-aqueous Li^+ electrolyte

Thomas A. Galloway[a], Gary Attard[b], Laurence J. Hardwick[a,*]

[a] Stephenson Institute for Renewable Energy, Department of Chemistry, University of Liverpool, Liverpool, UK
[b] Department of Physics, University of Liverpool, Liverpool, UK

ARTICLE INFO

Keywords:
Oxygen reduction reaction
Lithium-oxygen battery
Cyclic voltammetry
Single crystals
Platinum

ABSTRACT

Cyclic voltammetry has been used to probe the initial stages of oxygen reduction and oxidation in lithium-containing dimethyl sulfoxide at well-defined Pt single crystal electrodes in order to elucidate any catalytic effects ascribable to surface structure. In contrast to previous work involving sodium-oxygen, lithium-oxygen studies did not yield any significant differences for reaction on the three basal planes of platinum. Rather, all three planes generated a similar voltammetric response. However, by judicious use of various potential sweep limits, the formation of superoxide together with both a "conformal" or surface adlayer of lithium peroxide (Li_2O_2) together with a "microcrystallite" surface Li_2O_2 phase was resolved. Voltammetric peak intensity versus sweep rate measurements confirmed that superoxide electrooxidation was diffusion limited whereas electrooxidation of the two Li_2O_2 phases displayed behaviour typical of a surface-confined process. Under steady-state conditions for the formation of superoxide, it was found that for both the conformal and microcrystallite Li_2O_2 phases, electrooxidation followed zero-order kinetics, pointing to the importance of free surface sites in facilitating these reactions. A marked change in the rate of Li_2O_2 formation was found to coincide with a coverage of 0.25 monolayers, as measured by the charge density of the conformal Li_2O_2 electrooxidation peak. We postulate that electron tunnelling through both the conformal Li_2O_2 layer and microcrystallites deposited on this surface layer coincides with this coverage and accounts for such behaviour. This phenomenon of electron tunnelling through single conformal and mixed conformal/microcrystallite structures should prove vitally important in governing the overall electrooxidation rate.

1. Introduction

Lithium-oxygen (Li-O_2) or lithium-air cells exhibit an attractive theoretical specific energy of 3505 Wh kg^{-1} [1,2,3], which makes them possible candidates for next-generation energy storage systems. The underlying redox processes at the positive electrode involve the reduction (during discharge) of dioxygen (O_2) leading to the formation of lithium peroxide (Li_2O_2) with its subsequent oxidation and removal from the electrode surface (during charge). The precise mechanisms of the oxygen reduction reaction (ORR) and the oxygen evolution reaction (OER) have been intensively studied over the past decade [3–5,6–10,11,12]. Significant variations in ORR and OER in relation to lithium-oxygen redox chemistry have been reported as a consequence of both the chemical nature and composition of the electrode and its morphology [7,13].

The use of single crystal electrodes in aprotic solvents is one approach to the deconvolution of the complex structural surface contributions made to both bulk and surface redox processes occurring at the Li-O_2 positive electrode in order that the reaction mechanism and the role of catalytically active surfaces may be elucidated. Recent work by ourselves demonstrated a preparation method that maintains the surface order and cleanliness of platinum (Pt) single crystal electrodes to enable their use in electrochemical studies using non-aqueous electrolytes [14]. The well-defined nature of the Pt single crystal surfaces provided new information relating to surface-specific reaction pathways for O_2 electrochemistry in the presence of Na^+.

Herein, we extend such studies to the adsorption properties and surface coverages of reaction intermediates during ORR and OER in the presence of lithium ions using dimethyl sulfoxide (DMSO)-based electrolytes. Because of the known rapid conversion of lithium superoxide (LiO_2) to Li_2O_2, it is essential that processes occurring in the initial stages of oxygen redox activity in the presence of Li^+ should be examined and, moreover, any electrocatalytic effects relating to structure–reactivity properties be fully investigated. By utilising well-

* Corresponding author.
E-mail address: hardwick@liverpool.ac.uk (L.J. Hardwick).

https://doi.org/10.1016/j.elecom.2020.106814
Received 15 July 2020; Received in revised form 14 August 2020; Accepted 14 August 2020
Available online 17 August 2020

defined single crystal electrodes, it was hoped that delineation of superoxide and peroxide pathways might be resolved and therefore lead to a more fundamental understanding of Li-O_2 cell electrochemistry.

2. Experimental

2.1. Chemicals

$LiClO_4$ (Aldrich) was dried under vacuum overnight at 90 °C and stored in an argon-filled glovebox. Dimethyl sulfoxide (DMSO) (ROMIL) was distilled to remove impurities, and then stored over molecular sieves (4 Å) (Alfa Aesar).

2.2. Single crystal preparation

Pt hemispherical bead single crystals were prepared using Clavilier's method [15] and brought into the glove box for cell preparation as described in detail in [14].

2.3. Electrochemical measurements

Electrochemical experiments were conducted using a potentiostat (Biologic) in an argon glovebox and an in-house glass cell. Dry oxygen and argon gas lines were used to bubble and purge electrolytes, with water contents of < 20 ppm. All potentials were measured vs. Ag/Ag^+ pseudo reference. Potentials were then calibrated with an internal Fc/Fc^+ couple (0.68 V vs. SHE) and finally adjusted from Fc/Fc^+ to Li/Li^+ potential scale.

3. Results and discussion

3.1. Oxygen redox peaks in lithium-cation-containing electrolyte as a function of potential

Fig. 1(a) shows the voltammetric response of the three basal plane Pt electrodes to oxygen-saturated 0.1 M $LiClO_4$ in DMSO electrolyte. In contrast to results obtained in the presence of sodium cations [14], only minimal differentiation between the three Pt{hkl} terraced electrodes is observed during oxygen reduction. For example, both the onset of ORR at 2.73 V and the peak potential for the OER at 3.02 V are independent of the surface structure. There are minor variations in the magnitudes and overall shapes of the ORR and OER peaks, with Pt{1 1 1} giving rise to a slightly broader ORR peak than the other two planes. There are also some differences positive of the 3.02 V peak, with Pt{1 1 0} giving rise to a slightly larger OER charge. Overall, however, it is evident that whatever surface structural sensitivity there may be, it is a second-order effect and hence it is concluded that the same reaction mechanism is occurring on all Pt single crystal electrode surfaces. Similar CV responses have been observed on other substrates such as glassy carbon [16] and may reflect the dominance of solution phase Li-O_2 reactions relative to surface processes [3,10]. In order to explore this point further, Fig. 1(b) shows a potential window opening experiment using a Pt {1 1 1} electrode (analogous data for Pt{1 1 0} is shown in Fig. S1).

By systematically changing the negative potential limit, it is revealed that there is another redox process occurring on the positive-going sweep which is not observed in Fig. 1(a). We ascribe this peak at 2.58 V to the oxidation of residual lithium superoxide (LiO_2) formed in the previous negative-going sweep [6,7,10]. The superoxide peak intensity reaches a maximum for a negative potential excursion to 2.44 V and then diminishes as the potential limit becomes still more negative. This phenomenon is associated with the increasing conversion of LiO_2 to Li_2O_2 at more negative potentials such that on the reverse sweep no superoxide oxidation can be detected [6,7,10]. Instead, the growth in the 3 V peak is ascribed to oxidation of a Li_2O_2 species. The 3 V peak itself goes through an intensity maximum for a potential excursion at 2.14 V and at this point gives rise to an electrosorption charge of 977 μC

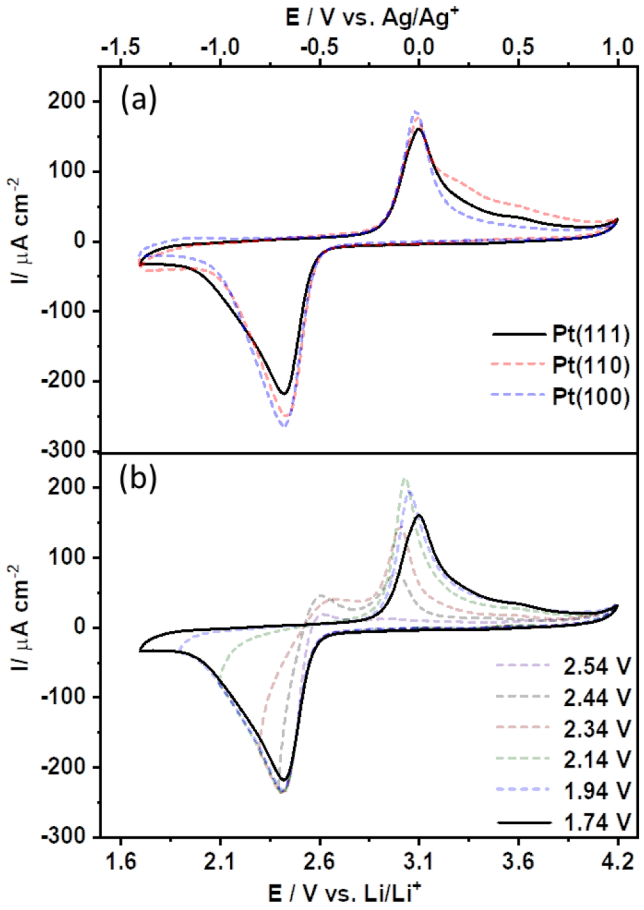

Fig. 1. Cyclic voltammetry in an oxygen-saturated electrolyte of 0.1 M $LiClO_4$ in DMSO at 50 mV/s (a) Pt{hkl} surfaces, (b) potential window opening on Pt {1 1 1}.

cm^{-2}. Since this peak should correspond to a two-electron electrooxidation of Li_2O_2 to oxygen gas and lithium cations, assuming that it is a surface process (see later), one may evaluate a nominal surface coverage of two monolayers (assuming 480 μC cm^{-2} corresponds to 1.5×10^{15} lithium peroxide molecules per cm^2).

One may also expect that electron tunnelling, required to facilitate electrooxidation of Li_2O_2, should also become limited, given the insulating nature of the material [17,11,18], such that as coverage of surface Li_2O_2 increases, an overpotential for electrooxidation should develop. This may be the reason for the subsequent shift to more positive potentials of the 3.02 V peak and its diminution for increasingly negative potential limits. Previous studies have determined that in fact two types of Li_2O_2 may be formed in Li-O_2 electrochemical cells depending on time, potential and solvent properties [12]. The first is a so-called "conformal" surface phase generated as a direct result of surface reduction of LiO_2 to give a relatively thin, surface-confined monolayer of Li_2O_2. In contrast, massive crystals of Li_2O_2 may form in the electrolyte via electroreduction of superoxide anions (O_2^-) or disproportionation of LiO_2. These large, "toroidal" microcrystallites may subsequently precipitate out onto the surface of the electrode [12]. Hence, the question of which type of Li_2O_2 might be forming on Pt {1 1 1} under our conditions is immediately raised. It should be noted from Fig. 1 that the 3 V peak is actually situated on an increasing base of charge which is clearly observed at more positive potentials and which also increases as the potential sweep limit becomes more negative. In order to address the nature of the Li_2O_2 species being formed, further cyclic voltammetry measurements were undertaken.

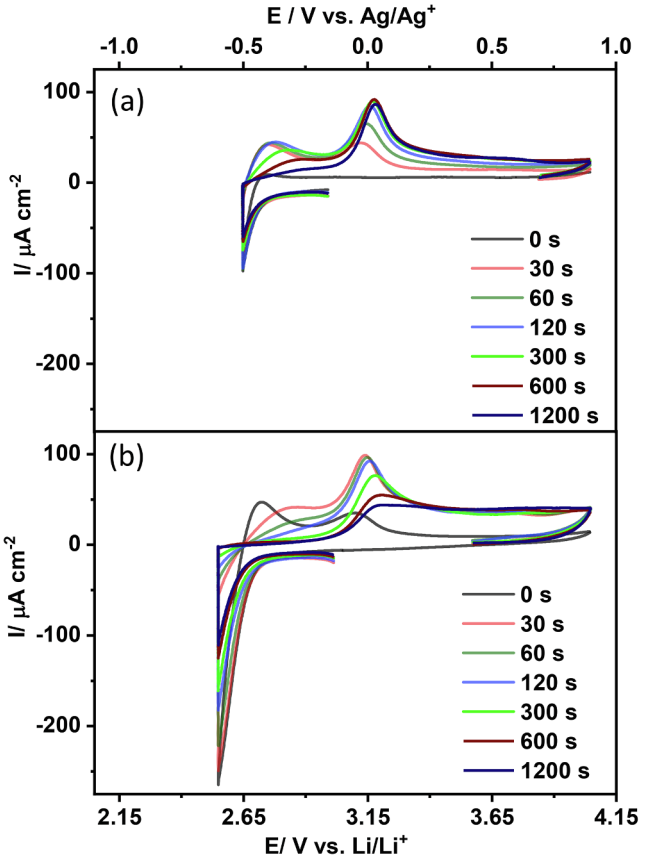

Fig. 2. Cyclic voltammetry of Pt{1 1 1} in an oxygen-saturated electrolyte of 0.1 M $LiClO_4$ in DMSO at 50 mV/s. The negative limit of holding potential is equal to (a) 2.65 V and (b) 2.55 V. Time period of potential holding is indicated in the figure.

3.2. Oxygen redox peaks in lithium-cation-containing electrolyte as a function of time

In Fig. 2, the effect of holding time on the oxidation peaks associated with LiO_2 and Li_2O_2 is explored at fixed potential. Holding at 2.65 V (Fig. 2(a)) reveals that at 120 s, the LiO_2 oxidation peak intensity reaches a maximum then falls to negligible levels after 1200 s. After holding for 0 s at the same potential, it is noted that no discernible oxidation peaks are observed on the positive-going sweep. Evidently, the amount of superoxide anion being formed under these conditions is negligible.

Again, we ascribe this behaviour to the formation of superoxide followed by subsequent consumption of this species in a second reduction and/or disproportionation process giving rise to Li_2O_2, which is observed in the oxidation peaks at 3 V together with "capacitive" charge at more positive potentials. At 30 s, both superoxide and peroxide oxidation peaks are comparable in size but after this point rapid formation of peroxide and the disappearance of superoxide is observed. In Fig. 2(b), the holding potential is made more negative (2.55 V). Overall, the consequence of this change is a similar rise and fall in the superoxide oxidation peak and *vice versa* for the peroxide oxidation peak. However, there are differences such as the rapid attenuation of the 3 V peak intensity after only 30 s holding time, leading to only "capacitive" charge features after 1200 s (current density plateau region from 3.1 to 4 V). We suggest that this "capacitive" charge is associated with the electrooxidation of the large, toroidal Li_2O_2 microcrystallites since it is known that Li_2O_2 oxidation takes place at the interface between the electrode and the Li_2O_2 [19]. If this process is inhibited (for example when oxidation needs to occur at relatively large distances away from the electrode surface, as would occur for large toroidal crystals of Li_2O_2) one should expect a larger overpotential and this indeed is the case for all charge transfer positive of about 3.1 V. However, for a surface-confined "conformal" layer, this process should be much faster and occur at a lower potential since there is a much more intimate contact between the Li_2O_2 film and the electrode surface with electron tunnelling distances being relatively small. Indeed, it is speculated that this surface layer (directly in contact with Pt atoms) might restructure significantly from the normal Li_2O_2 crystal structure, leading to enhanced conductivity. In fact, the generation of an initially amorphous and electronically distinct bulk Li_2O_2 phase together with the subsequent formation of a more crystalline Li_2O_2 phase has been observed previously [2]. However, due to the relatively small amount of oxidation charge passed at 3 V in our case, we suggest that the association of this electrochemical feature with a surface phase is more appropriate. Therefore, based on this idea, it is plausible to ascribe the 3 V peak to lithium peroxide formed exclusively at the surface of the electrode via reduction of lithium superoxide rather than from disproportionation of lithium superoxide formed in the bulk of the electrolyte. Within this model, the attenuation in the magnitude of the 3 V peak would occur as the thickness of the conformal layer increased such that it too gave rise to an oxidation overpotential commensurate with the large toroidal crystallites that deposit onto the electrode surface at high local concentrations of LiO_2. Hence, both Figs. 1 and 2 may be seen as reflecting the relative amounts of superoxide, conformal lithium peroxide (3 V peak) and toroidal lithium peroxide (charge passed positive of 3.1 V) that are formed depending on potential or holding time at a given potential. The well-defined structure of the Pt{1 1 1} surface makes all of these voltammetric features more readily resolved than in previous studies [6].

3.3. Peak sweep rate dependence of lithium superoxide and peroxide peaks

Typical data for the dependence of peak intensity on sweep rate for the three oxidation peaks highlighted previously were collected at a fixed holding potential of 2.59 V followed by sweeping positive at a series of different sweep rates (Fig. S2). When the intensity of the superoxide oxidation peak was plotted against the square root of the sweep rate, a linear trend was observed, attesting to the oxidation kinetics being under diffusion control. This is consistent with residual LiO_2 being accumulated in the bulk of the electrolyte following reaction of superoxide anions with lithium cations and is in accordance with previous investigations [3,10]. However, in contrast, both the 3 V peak and the "capacitive" charge positive of this feature show a linear dependence on sweep rate, confirming that the oxidation in each case is a surface process, consistent with our previous assumptions that both are indeed surface redox reactions.

Taking into account the discussion thus far together with previous studies of Li-O_2 electrochemistry [3,10,12,20], Scheme 1 illustrates a consistent overview of the overall redox and disproportionation reactions taking place.

Although at first glance rather complex, Scheme 1 simply consists of a number of sequential one-electron transfers both at the surface (equations 1–3) and in the electrolyte solution (equations 1′–3′) together with a pair of two-electron transfers involving direct surface electrooxidation of lithium peroxide to dioxygen with equation 5 associated with electrooxidation of the conformal lithium peroxide phase and equation 6 (at greater overpotentials) corresponding to electrooxidation of large toroidal microcrystallites of Li_2O_2. Equation 5 may formally be considered as the reverse of equations 3, 2 and 1 and simply reflects our uncertainty concerning whether a single two-electron transfer or consecutive one-electron transfers are occurring. Equations 4 and 4′ are included in order to cover the possibility of lithium peroxide formation via disproportionation of lithium superoxide on the surface and in the electrolyte phase, leading also to the formation of singlet oxygen as a reaction product [21]. In order to keep the

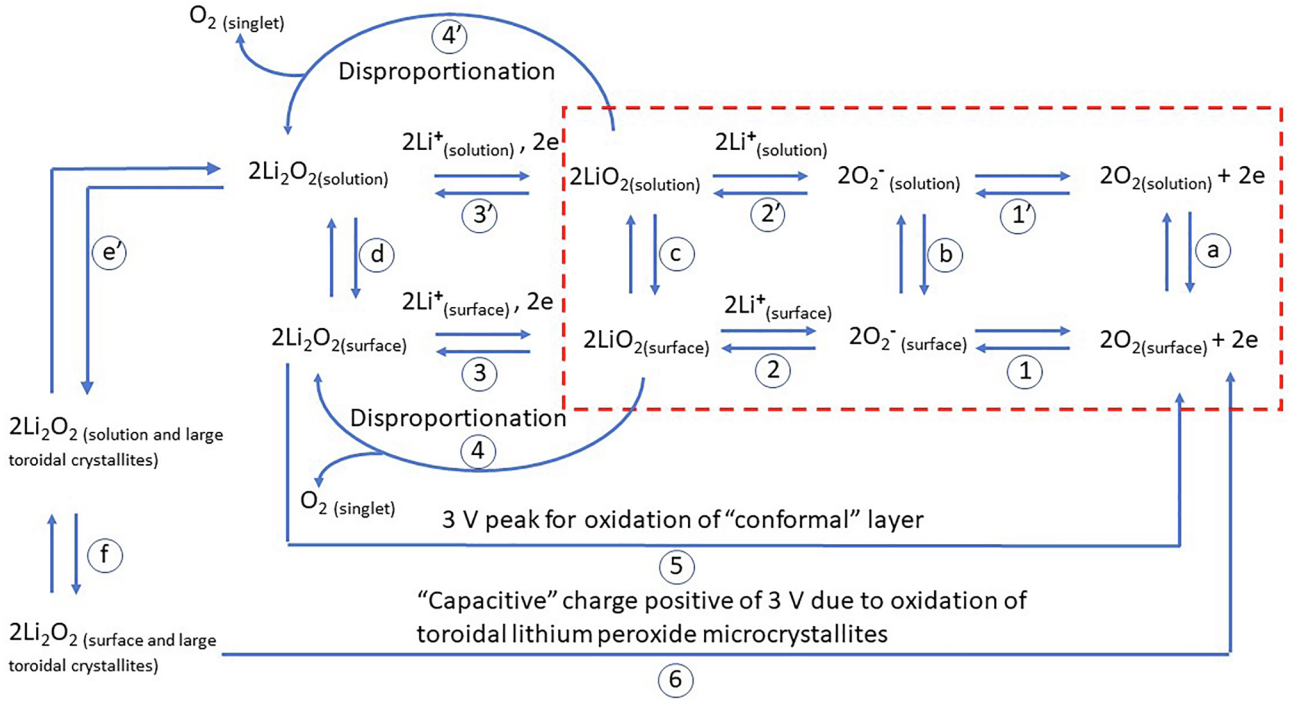

Scheme 1. Reaction pathways during ORR and OER in the presence of lithium cations.

mechanism quite general and to also acknowledge the significant role of solubility of reaction intermediates in DMSO [10], equations a–d and f represent solubility equilibria of surface species with the electrolyte and equation e′ corresponds to the nucleation and growth of lithium peroxide nuclei into massive crystallites in solution.

3.4. Kinetic studies of lithium peroxide oxidation on platinum

In order to address further aspects concerning the relative rates of formation of both conformal and toroidal surface phases, one may take advantage of the ease with which one may form soluble superoxide species via control of the potential. For example, Fig. 1(b) and 2 reflect an "overproduction" of superoxide species, allowing all reactions in Scheme 1 to occur readily. However, if one "throttles back" on the formation of superoxide by making the overpotential for oxygen reduction less negative, it may be possible to ensure a constant but *limited* concentration of superoxide. This essentially generates a steady-state concentration of superoxide and is represented in Scheme 1 by the equations contained within the dotted rectangle. Hence, under such conditions the growth in lithium peroxide is limited purely by the supply of superoxide species to the system. Measurement of the 3 V conformal peak and the charge associated with surface toroidal crystallites would then reflect the rates of equations 3 and 3′/4′, respectively. Fig. 3 shows voltammetric data satisfying the conditions described above with a constant superoxide oxidation peak intensity and a corresponding growth in the oxidation peaks associated with Li_2O_2. It should be noted that such conditions could not be satisfied using polycrystalline Pt at *any* negative potential limit. We suggest that the large number of different adsorption sites, each having its own overpotential for superoxide generation, precluded the maintenance of steady-state conditions in the formation of superoxide.

From Fig. 3 the holding potential of 2.66 V facilitated the growth of conformal Li_2O_2 via equation 3 in Scheme 1 together with toroidal Li_2O_2 via equations 3′, 4′, e′ and f. A plot of charge versus time for the 3 V peak is shown in Fig. S3. The initial growth kinetics clearly correspond to zero-order kinetics since a linear relationship between surface coverage (charge) and time is obtained. Since the rate of reaction is independent of reactant concentration, the only factor that affects

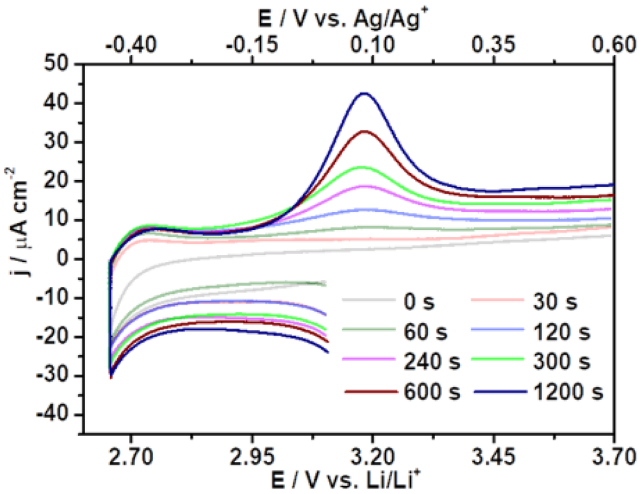

Fig. 3. Generation of surface lithium peroxide phases at constant (low) concentrations of lithium superoxide on Pt{1 1 1}. The holding potential used was 2.66 V. After this, the potential sweep was engaged at 3.15 V towards more negative potentials and then swept positive from 2.66 V.

equation 3 must be the availability of Pt sites, as these catalyse the reaction. Zero-order reactions are typically found when a material that is required for the reaction to proceed, such as the surface of a catalyst, is saturated by the reactants, in this case superoxide anions and lithium cations [22].

However, it is also clear from Fig. S3 that there are actually two linear sections to the plot which intersect at a charge density of ca. 120 μC cm^{-2}. For a two-electron transfer, this would reflect a nominal surface coverage of lithium peroxide of 120/480 = 0.25 monolayers. Hence, if zero-order kinetics are maintained even in the latter stages of growth of the conformal layer, the slowing of the rate could be due to the fact that electron tunnelling is now occurring through both the conformal layer and Li_2O_2 subsequently deposited onto these structures. This would signify that second-layer growth of Li_2O_2 was commencing prior to completion of the first monolayer under these

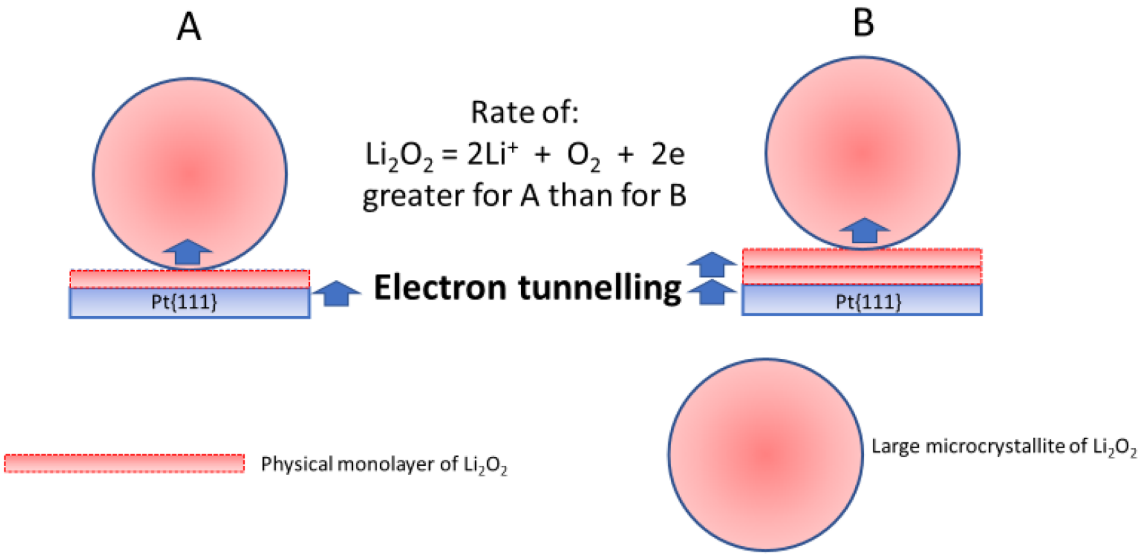

Fig. 4. Schematic explanation of why a marked change in the electrooxidation kinetics of both surface lithium peroxide and macroscopic lithium peroxide crystals occur in terms of conformal surface layer/microcrystallite thickness and its effect on electron tunnelling.

conditions. It is interesting that when the current density at 3.67 V (a descriptor of toroidal Li_2O_2 growth and coverage) is plotted, a similar graph to Fig. S3 is observed with a linear dependence of current density on time and a similar sharp break in the gradient coinciding with the time of second and subsequent layer growth on top of the conformal layer (see Fig. S4). We explain this phenomenon in terms of toroidal microcrystals sitting on top of the conformal layer (Fig. 4). Thus, electron transport through the conformal layer will control any subsequent oxidation reaction taking place on the large Li_2O_2 microcrystallites sitting proud of the surface. This is consistent again with redox processes for Li_2O_2 being limited to the interfacial region between Li_2O_2 and the surface of the electrode.

Finally, in Fig. S5 a holding potential of 2.73 V is utilised such that only minimal production of superoxide anion is occurring. In this case, no conformal lithium peroxide peak is obtained upon sweeping the potential. There is an increase in the double-layer capacitive current with time which we ascribe to the oxidation of Li_2O_2 crystallites formed solely from disproportionation of LiO_2 in the electrolyte which subsequently deposit on the electrode surface. It is noted that even here, the current densities associated with oxidation are very low compared to those in Fig. 3. This experiment suggests that it may be possible to form Li_2O_2 microcrystallites at the surface of an electrode without the corresponding formation of a conformal layer, presumably because the potential for conversion of surface superoxide into surface peroxide is more negative than that for superoxide formation and subsequent disproportionation. This is in accord with previous studies by Shao-Horn et al. [12].

4. Conclusion

Cyclic voltammetry (CV) studies on the three basal planes of platinum of non-aqueous ORR and OER in the presence of lithium cations and DMSO solvent did not yield any substantial variances. Nevertheless, resolution of surface Li_2O_2 phases was achieved via careful control of potential sweep limits and potential holding CV sweeps. The study confirmed that superoxide electrooxidation was a diffusion-limited process whereas electrooxidation of the two Li_2O_2 phases was a surface-confined process. Under steady-state conditions for the formation of superoxide, it was found that for both the conformal and microcrystallite Li_2O_2 phases electrooxidation followed zero-order kinetics, pointing to the importance of free surface sites in facilitating these reactions.

CRediT authorship contribution statement

Thomas A. Galloway: Visualization, Writing - original draft, Investigation, Formal analysis, Validation, Methodology, Conceptualization. **Gary Attard:** Supervision, Visualization, Writing - review & editing, Writing - original draft, Formal analysis, Methodology, Conceptualization. **Laurence J. Hardwick:** Funding acquisition, Project administration, Supervision, Visualization, Writing - review & editing, Writing - original draft, Formal analysis, Conceptualization.

Declaration of Competing Interest

The authors declare that they have no known competing financial interests or personal relationships that could have appeared to influence the work reported in this paper.

Acknowledgment

Support from Engineering and Physical Sciences Research Council (EP/R020744/1) is gratefully acknowledged.

Appendix A. Supplementary data

Supplementary data to this article can be found online at https://doi.org/10.1016/j.elecom.2020.106814.

References

[1] P.G. Bruce, S.A. Freunberger, L.J. Hardwick, J.M. Tarascon, Nat. Mater. 11 (2012) 19–29.
[2] D. Aurbach, B.D. McCloskey, L.F. Nazar, P.G. Bruce, Nat. Energy 1 (2016) 16128.
[3] T. Liu, J.P. Vivek, E.W. Zhao, J. Lei, N. Garcia-Araez, C.P. Grey, Chem. Rev. 120 (2020) 6558–6625.
[4] J.P. Vivek, N.G. Berry, J. Zou, R.J. Nichols, L.J. Hardwick, J. Phys. Chem. C 121 (2017) 19657–19667.
[5] J.P. Vivek, N. Berry, G. Papageorgiou, R.J. Nichols, L.J. Hardwick, J. Am. Chem. Soc. 138 (2016) 3745–3751.
[6] Z. Peng, S.A. Freunberger, L.J. Hardwick, Y. Chen, V. Giordani, F. Bardé, P. Novák, D. Graham, J.-M. Tarascon, P.G. Bruce, Angew. Chemie Int. Ed. 50 (2011) 6351–6355.
[7] T.A. Galloway, L.J. Hardwick, J. Phys. Chem. Lett. 7 (2016) 2119–2124.
[8] S.A. Freunberger, Y.H. Chen, Z.Q. Peng, J.M. Griffin, L.J. Hardwick, F. Barde, P. Novak, P.G. Bruce, J. Am. Chem. Soc. 133 (2011) 8040–8047.
[9] N. Mahne, B. Schafzahl, C. Leypold, M. Leypold, S. Grumm, A. Leitgeb, G.A. Strohmeier, M. Wilkening, O. Fontaine, D. Kramer, C. Slugovc, S.M. Borisov,

S.A. Freunberger, Nat. Energy 2 (2017) 17036.
[10] L. Johnson, C. Li, Z. Liu, Y. Chen, S.A. Freunberger, P.C. Ashok, B.B. Praveen, K. Dholakia, J.-M. Tarascon, P.G. Bruce, Nat. Chem. 6 (2014) 1091–1099.
[11] B.D. McCloskey, D.S. Bethune, R.M. Shelby, T. Mori, R. Scheffler, A. Speidel, M. Sherwood, A.C. Luntz, J. Phys. Chem. Lett. 3 (2012) 3043–3047.
[12] D.G. Kwabi, M. Tułodziecki, N. Pour, D.M. Itkis, C.V. Thompson, Y. Shao-Horn, J. Phys. Chem. Lett. 7 (2016) 1204–1212.
[13] C.J. Bondue, P. Reinsberg, A.A. Abd-El-Latif, H. Baltruschat, PCCP 17 (2015) 25593–25606.
[14] T.A. Galloway, J.-C. Dong, J.-F. Li, G. Attard, L.J. Hardwick, Chem. Sci. 10 (2019) 2956–2964.
[15] J. Clavilier, R. Faure, G. Guinet, R. Durand, J. Electroanal. Chem. Interfacial Electrochem. 107 (1980) 205–209.
[16] V.S. Dilimon, D.-G. Lee, S.-D. Yim, H.-K. Song, J. Phys. Chem. C 119 (2015) 3472–3480.
[17] M.D. Radin, D.J. Siegel, Energy Environ. Sci. 6 (2013) 2370–2379.
[18] M.O. Thotiyl, S.A. Freunberger, Z.Q. Peng, P.G. Bruce, J. Am. Chem. Soc. 135 (2013) 494–500.
[19] Q. Peng, J. Chen, H. Ji, A. Morita, S. Ye, J. Am. Chem. Soc. 140 (2018) 15568–15571.
[20] N. Mahne, O. Fontaine, M.O. Thotiyl, M. Wilkening, S.A. Freunberger, Chem. Sci. 8 (2017) 6716–6729.
[21] E. Mourad, Y.K. Petit, R. Spezia, A. Samojlov, F.F. Summa, C. Prehal, C. Leypold, N. Mahne, C. Slugovc, O. Fontaine, S. Brutti, S.A. Freunberger, Energy Environ. Sci. 12 (2019) 2559–2568.
[22] L. Arnaut, S.J. Formosinho, H. Burrows, Chemical Kinetics, Elsevier, 2006.